RSC Sustainability

ROYAL SOCIETY OF CHEMISTRY

TUTORIAL REVIEW

View Article Online
View Journal | View Issue

Cite this: *RSC Sustainability*, 2023, **1**, 1952

Recent advances in Cu-BTC MOF-based engineered materials for the photocatalytic treatment of pharmaceutical wastewater towards environmental remediation

Saptarshi Roy, Jnyanashree Darabdhara and Md. Ahmaruzzaman *

Water-borne emerging pollutants are among one of the serious issues facing modern society. As a result of the excessive consumption of drugs during the global COVID-19 pandemic, a huge number of pharmaceuticals and personal care products are widely dispersed into aqueous sources and may pose serious health issues to all life forms, besides destroying the ecosystem. Treatments of these toxic and persistent pharmaceutical contaminants in wastewater effluents have received widespread attention from researchers devoted to environmental remediation. Metal organic frameworks (MOFs) and their composites have been reported to be effective materials for such applications. This review is devoted to providing a brief outline by compiling the various advantageous features of Cu-BTC MOF, focusing on the synthesis, reactivity and its recent potential applications in the field of elimination of toxic pharmaceutical wastes and personal care products from wastewater effluents. Moreover, it documents the mechanistic pathway involved in the degradation mechanism and paints the various limitations and future research outlooks that may be helpful by considering the current scenario to fully comprehend and exploit the potentiality of this promising nanostructural framework.

Received 11th August 2023
Accepted 13th September 2023

DOI: 10.1039/d3su00276d

rsc.li/rscsus

Sustainability spotlight

The quick growth of industry has made environmental degradation a serious global issue. All living things are at risk to health owing to water pollution, which is an urgent concern in the modern world. Millions of tons of pharmaceuticals and drugs have been manufactured and sold for various consumer, agricultural and industrial applications. The frequent discovery of these persistent and hazardous pharmaceuticals in wastewater effluents has sparked global concerns about the possible long-term consequences on aquatic organisms and human health besides affecting the ecosystem at large. The large-scale utilization of conventional photocatalysts, such as ZnO, TiO_2, and ZnS, is limited because the photocatalysis efficiency is particularly hindered by the rapid recombination of photogenerated electron–hole pairs, low efficiency of solar energy utilization and limited surface active sites. In contrast, MOFs offer distinctive features, such as tunable porosity, high specific surface area and open frame structure, that facilitate the diffusion of pollutants to the active sites of the catalyst. Moreover, the functionalization of MOFs can regulate the spectral response range, making them well-suited for constructing composite catalytic materials by integrating with other active materials. Cu-MOF has garnered significant attention in recent years because of its exceptional properties, which include remarkable thermal stability, large surface area, and substantial pore volume. Notably, the presence of redox active Cu^{2+} ions enhances its effectiveness in photocatalysis by participating in both oxidation and reduction reactions. Additionally, it exhibits impressive structural integrity during the adsorption–desorption of water. As heterogeneous and recyclable photocatalysts, Cu-MOFs offer a sustainable approach to pharmaceutical removal by employing solar energy to drive the degradation reactions, reducing the need for energy-intensive conventional treatment methods and contributing to the development of environmentally friendly technologies. Photocatalytic degradation of these toxic compounds by MOF candidates offers a promising approach for efficiently removing these pollutants from wastewater, thereby minimizing their release into natural water systems and achieving sustainable development goals.

1. Introduction

Environmental contamination is one of the most formidable issues threatening human existence and advancement in the present century because of rapid industrial evolution. This has led to the increased generation of waste and the release of these chemicals into water resources as a result of insincere human activities.[1,2] Majority of the global population lacks access to clean drinking water, which is a crucial element in the existence of life on earth. Therefore, it has become essential for the scientific community to discover sustainable ways to eliminate these contaminants from the industrial effluent before discharging them into the environment.[3] Solar energy is a viable option among the various energy sources because of its clean and abundant nature. Consequently, solar-light-powered technologies have garnered increased interest from researchers owing to their practical applications in environmental

Department of Chemistry, National Institute of Technology Silchar, 788010, Assam, India. E-mail: mda2002@gmail.com

remediation. Thus, semiconductor-based photocatalytic systems have received widespread acceptance as prospective materials owing to their intriguing features of high stability and efficiency, cost-effectiveness, minimal toxicity and chemical inertness. Despite being the most extensively exploited and representative photocatalytic material, the efficiency of TiO_2 is restricted because of its activation by visible light, making it easy for the photogenerated electrons and holes produced under illumination to recombine with one another. Moreover, single-component nano TiO_2 catalysts suffer drawbacks, including a low rate of pollutant degradation, easy aggregation of the particles and difficulty in recycling. Again, successful migration and the separation of charge carriers depend greatly on rational engineering through semiconductor heterostructure morphology.[4,5] Hence, there is a pressing need to develop highly active and stable visible light responsive photocatalysts for future large-scale practical utilization.

Metal–organic frameworks (MOFs) have emerged as a unique and novel class of microporous materials constituting metal ions and organic building blocks.[6–8] They are organized by coordination interactions between the linker molecules and metal ions and hence are termed porous coordination polymers. These inorganic–organic hybrid materials have captured the interest of the global scientific community in the realm of photocatalysis because of their impressively high specific surface area and crystallinity, diverse topology, thermal and mechanical stability and tunable porous structure.[9–11] Moreover, using defect engineering and linker modification approaches, it is possible to introduce catalytically active sites because of the interesting adaptability of MOF structures.[12] Additionally, as isolated semiconductor QDs and light-absorbing antennas, metallic-oxo clusters and organic ligands impart MOFs with semiconductor-like characteristics. Different periodic structures and porosities are determined by the distinctive coordination geometry of metals and ligands.[2,13] It is possible to tailor MOFs with unique features by selecting efficient organic linkers and metal ions for the better utilization of visible light. With the development of MOFs that are resistant to water and acidic conditions, various light-responsive MOFs have been fabricated for a diverse range of applications, including drug delivery, photocatalytic elimination of pollutants, bioimaging, gas separation, gas adsorption and storage, generation of H_2, CO_2 fixation, energy storage, and selective heterogeneous catalysis.[6,14–17]

Numerous reviews that have discussed the various aspects of MOFs, including their practical utility in environmental remediation, have been published in the last decade. However, few articles have specifically addressed Cu-BTCMOF, particularly for environmental applications. However, to the best of the author's knowledge, no such review focusing on the elimination of pharmaceutical wastes from aqueous sources for environmental remediation has yet been reported. Finally, this article provides a brief overview of various advantageous features of Cu-BTC MOF by focusing on the various synthetic approaches, reactivity and its recent potential application in the field of elimination of toxic pharmaceutical wastes and personal care products from wastewater effluents. It also elaborates on the mechanistic pathway involved in the degradation mechanism and presents various limitations and future research outlooks that may be helpful in fully comprehending and exploiting the potentiality of this promising nanostructural framework.

2. Background of the Cu-BTC MOF

Copper benzene 1,3,5-tricarboxylate, also commonly known as HKUST-1, $Cu_3(BTC)_2$ or MOF-199, is a versatile material that finds its applications in various fields owing to its extremely porous, stable and high surface area characteristics.[18,19] It has a paddlewheel type of geometry composed of copper nodes interconnected by 1,3,5-benzenetricarboxylic acid (BTC) and was first reported by Chui and his co-workers in 1999. Fig. 1 illustrates the structure of HKUST-1 MOF in which two Cu^{2+} metal ions are coordinated to four carboxylate groups in the paddlewheel structure to form a three-dimensional porous network with the chemical formula $[Cu_3(BTC)_2(H_2O)_3]_n$.[20,21] Additionally, in the hydrated state, one molecule of H_2O coordinates with the two metal centres in the axial position.

3. Advantages of Cu-BTC MOF

HKUST-1 MOF is a nanoporous material with interesting features that make it a promising candidate for various practical applications.[22,23] They are endowed with several advantageous characteristics that make them superior materials for photocatalytic applications over traditional nanomaterials. Some of the properties worth mentioning are as follows:

(i) High surface area: because of its porous structure, HKUST-1 offers a significantly large surface area and greater active sites, resulting in improved reaction with the pollutant molecules in photocatalytic degradation.

(ii) Tunable properties: the structure of the HKUST-1 MOF can be altered by the choice of suitable metal ions and organic linkers, allowing scientists to tailor properties suitable for specific reaction mechanisms and conditions.

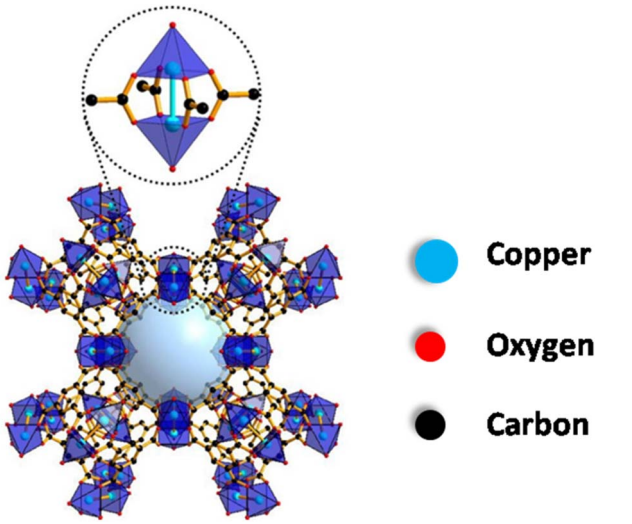

Fig. 1 Structure of HKUST-1 MOF. Reproduced from ref. 20.

(iii) High stability: HKUST-1 maintains good thermal and chemical stability, which is essential for preserving its photocatalytic efficiency over repeated cycles, especially under harsh reaction conditions.

(iv) Response to visible light: the distinctive electronic structure of HKUST-1 allows it to respond to visible light in contrast to many conventional photocatalysts that primarily absorb UV light. Consequently, it can be employed in a wide range of practical applications, as visible light makes up a significant portion of the solar spectrum.

(v) Functionalization: HKUST-1 can be easily functionalized with various organic groups, which broadens its potential utility.

(vi) Effective charge separation: the capability to effectively separate photogenerated charge carriers is one of the essential characteristics of a potential photocatalyst. This charge separation can be easily facilitated by HKUST-1, thereby improving its photocatalytic activity.

(vii) Pore size control: the possibility of regulating pore size at the molecular level makes it a promising catalyst for applications, including selective gas adsorption.

(viii) Versatility: the HKUST-1 MOF is versatile and can be employed for various applications, such as photocatalytic degradation of contaminants, production of H_2 from water splitting, CO_2 reduction, gas storage, drug delivery, and catalysis. It is suited to an extensive range of applications owing to its tunable features and stable framework.

(ix) Reusability: the stability of the HKUST-1 framework offers it the potential to be recycled and reused for several cycles without a significant reduction in catalytic efficiency. This lowers the frequency of material replacement, making it a cost-effective catalyst.

4. Synthetic approaches

Many synthetic approaches have been reported for synthesizing Cu-BTC composites. Herein, we summarize recent studies showcasing various methods for the preparation of composites.

4.1. Solvothermal approach

The solvothermal approach is the most extensively employed method for synthesizing Cu-BTC MOF in a liquid phase. This involves the continuous stirring of H_3BTC in a mixed solvent of BnOH : ethanol (15 : 1) and metal ions maintained at a predetermined temperature of 80 °C for 3 h.[24,25] The subsequent filtration of the reaction mixture, along with solvent evaporation, finally yields pure MOF crystals. Qiao *et al.* proposed a yolk–shell nanoreactor based on TiO_2@HKUST-1 by applying a three-step synthetic route,[24] as demonstrated in Fig. 2. First, homotarboxylic acid was homogeneously dispersed in a solution of benzyl alcohol and ethanol to which a solution of TiO_2@Cu_2O was added. The reaction was allowed to continue for 2 h and then settle. Finally, the precipitate was washed with CH_3OH many times, followed by heating at 80 °C for 12 h. Again, Cu_2O@HKUST-1 heterostructure with three different geometries was synthesized by Wu *et al.* by adding Cu_2O in an alcoholic solution of H_3BTC, followed by stirring at 80 °C in a water bath for 3 h.[25,26] It was then washed with water and ethanol and subsequently vacuum dried at 60 °C. Another procedure involves the preparation of a homogeneous solution of organic linkers in a 1 : 1 : 1 mixture of DMF, EtOH and water, followed by the addition of $Cu(OAc)_2 \cdot H_2O$ and triethylamine to the aforementioned solution.[27,28] It was then agitated for 23 h, centrifuged, washed and dried at 100 °C. Again, SnO_2/MOF-199 (HKUST-1) nanocomposite was prepared using a solvothermal approach by introducing different mass ratios of SnO_2 to MOF-199 to evaluate the degradation performance of metronidazole (MZ).[27] The reaction mixture was then refluxed for 4 h, washed and finally dried at 353 K in vacuum. Hydrothermal synthesis is regarded as one of the environment friendly approaches for the synthesis of HKUST-1 because it employs water rather than other potentially hazardous organic solvents. In this method, a combination of organic ligands, metal ions and solvents is placed inside a Teflon-coated autoclave and heated at a specific temperature.[29] After the termination of the reaction, the reactor is cooled to room temperature, and the resulting product is washed and vacuum dried. This technique is particularly valuable for generating MOFs with controlled crystal size and symmetry although it tends to yield a comparatively lower amount of product. Although various MOFs have been designed, the need for a facile, convenient and environmentally benign approach that results in a superior crystalline framework remains. Morales and his team, for the first time, successfully synthesized HKUST-1 by employing a reactor Monowave 50 (Anton Paar) using a non-conventional solvothermal technique.[30] Instead of long durations of 10 to 24 h, this novel approach minimizes the reaction time to about 15 min, maintaining an attractive monocrystalline nanostructure that opens its scope for various potential applications.

4.2. Microwave-assisted synthesis

The microwave-assisted synthesis offers a significantly accelerated method for the preparation of HKUST-1 compared to the hydrothermal approach by reducing the synthesis time from 24 h to just 30 min. This technique enables the production of HKUST-1 with exceptional crystallinity, a well-defined porous structure, notably smaller particle size, and precise control over its morphology. It relies on the interaction between electromagnetic waves and molecules or ions of polar solvents, leading to the rapid formation of MOF. In a typical synthesis, an aqueous solution of Cu $(NO_3)_2 \cdot 6H_2O$ was introduced into an ethanolic solution of H_3BTC, transferred to a reactor and placed in a microwave synthesizer.[31–33] The reaction was conducted by heating it to 393 K for 20 min, after which it was cooled to room temperature and subsequently subjected to centrifugation and drying.

4.3. Sonochemical synthesis

The sonochemical method employs high-intensity ultrasonic waves within the frequency range of 20 kHz–10 MHz to induce chemical transformations in the reactants. The application of ultrasound leads to a phenomenon called cavitation, which

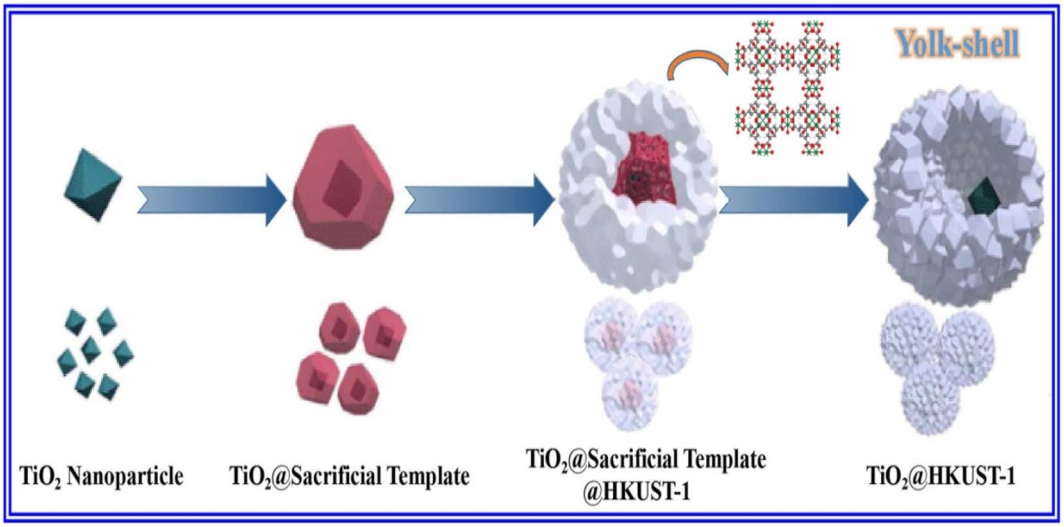

Fig. 2 Schematic exhibition for the fabrication of TiO_2@HKUST-1. Reproduced from ref. 24.

instigates both chemical and physical alterations in the substances involved. The process generates tiny bubbles within the liquid medium, forming localized hotspots upon collapse. These hotspots have a shorter lifespan but exhibit elevated temperature and pressure, resulting in the production of uniform nucleation sites. Consequently, this shortens the time needed for the crystallization process. Typically, the probe of the sonicator is immersed into a vial containing the reactants and solvents, causing a transformation from a clear blue precursor solution to the turbid slurry and yielding tiny HKUST-1 crystals.[34] These MOF crystals were rinsed with acetone and dried for further use.

4.4. Electrochemical synthesis

The electrochemical method differs from the conventional method because it eliminates the utilization of metal salts within the solution. Instead, this strategy relies on an electrode submerged in a solution containing the electrolyte and the organic linker. When voltage or current is applied, the electrode undergoes dissolution, releasing the metal ions necessary for the construction of the MOF. These liberated metal ions react promptly with the organic ligands present in the solution, leading to the immediate formation of the MOF close to the surface of the electrode.[35,36]

4.5. Mechanochemical synthesis

Also referred to as the grinding method, it produces MOFs by mechanical disturbance or collisions between the interacting reactants.[37] It is an energy-efficient green synthesis, uses relatively less solvent and does not entail the application of heat.[38,39] Moreover, the generation of water as a by-product makes it an environmentally benign procedure. It is a very simple, effective, and simple procedure for making MOFs.

Each of these approaches has its advantages and can be utilized depending on the desired MOF properties, the rate of the reaction, and the simplicity of scaling up. The choice of synthetic method also relies greatly on specific research objectives and the available types of equipment and resources.

5. Cu-BTC MOF-based photocatalysts for the photocatalytic elimination of pharmaceuticals and personal care products

Pharmaceuticals and personal care products (PPCPs) are recently emerging water contaminants that have caused global concern. This includes commonly used drugs, antibiotics, analgesics and daily essentials for personal hygiene. With the advent of civilization, there has been a tremendous increase in the manufacturing and consumption of these drugs. Because of their persistent and toxic nature, they tend to accumulate in the environment, causing acute environmental concerns. Additionally, it affects various life forms and causes mutations in the bacterial genes that produce drug-resistant pathogens. Therefore, it has become crucial to develop effective strategies for the degradation of PPCPs to safeguard our environment. To address this issue, MOF-based photocatalysts have been utilized as novel materials with significant research potential for the photocatalytic degradation of pharmaceuticals.[40]

Qiao *et al.* proposed a unique yolk–shell nanoreactor based on TiO_2@HKUST-1 with noticeably higher stability and photocatalytic efficacy for the elimination of TC under visible light.[24] The degradation efficiency of the TiO_2@HKUST-1 was found to be 92.40% within 60 min, which was significantly higher than its pristine counterparts. The designed nanoreactor structure effectively enhanced the interfacial contact that significantly led to the increase in specified surface area, carrier density and separation of photogenerated e^- and h^+, thereby increasing the photocatalytic efficiency. Further, Andrade and his co-workers studied the elimination of sodium diclofenac and ibuprofen and observed an increase in the degradation efficiency

compared to pure MOF.[41] Moreover, it was reported that cubic Cu_2O@HKUST-1 presented a higher degradation performance of tetracycline (TC-HCl) than truncated and octahedral Cu_2O@HKUST-1.[25,26] Mechanistic explorations revealed that octahedral Cu_2O@HKUST-1 exhibited type I heterojunction, resulting in the recombination of photogenerated charge carriers. In contrast, the existence of a type II heterojunction in cubic and truncated Cu_2O@HKUST-1 yielded effective separation and charge migration that subsequently led to an outstanding light response and photocatalytic performance towards the degradation of TC. The wide band gap energy and the huge rate of recombination of the photogenerated charge carriers restrict the utilization of $BaTiO_3$ as a photocatalyst in wide scale industrial applications. Several strategies have been developed in recent times by developing heterostructure composites with similar low band gap semiconductors to enhance their photocatalytic performance effectively. Inspired by these investigations, a series of $BaTi_{0.85}Zr_{0.15}O_3$/MOF-199 (HKUST-1) nanocomposites were fabricated by Sheikhsamany *et al.*[28] involving electrostatic interactions between the MOF and $BaTi_{0.85}Zr_{0.15}O_3$ for utilization in the photodegradation of TC. SnO_2 displays good chemical, optical and electrical characteristics besides offering other advantageous characteristics of complete mineralization, minimum operating cost and ambient functioning conditions. However, pristine SnO_2 is prone to corrosion and metal toxicity and is not very light and stable in aqueous conditions. In this regard, strategies involving the encapsulation of SnO_2 NPs in MOF cages have led to increased catalytic activity and stability of the photocatalyst, which has been utilized for the elimination of medicinal contaminants, such as MZ.[27] Typically, the HOMO of HKUST-1 lies at a higher positive value than that of the majority of MOFs, suggesting that the photogenerated h^+ displays a greater oxidation capability. This can be utilized to fabricate direct Z-scheme heterojunctions by integrating m-$BiVO_4$ and HKUST-1 to aid in the redistribution and separation of photo-generated charge carriers compared to single photocatalyst materials. Yuan *et al.* designed a HKUST-1@m-$BiVO_4$ catalyst that exhibited a maximum removal efficiency of 91.72% under visible light towards TC.[42] This can be attributed to the fairly good synergistic effect of the Cu^{2+}/Cu^+ fenton-like reaction and Z-scheme heterojunction, which can further aid in the formation of ROS under visible light in the degradation mechanism.

The widespread use of ciprofloxacin (CIP) as an antibiotic, constituting many healthcare and personal care products, livestock and fish farming, has resulted in contamination of the aqueous sources of our environment. It persists in our environment owing to its stable molecular structure and poor biodegradability. Elevated concentrations of CIP in the range of 150 μg L^{-1}–31 mg L^{-1} have been observed in hospital and pharmaceutical industry effluents. Therefore, it is of utmost importance to develop novel and highly potential strategies for eliminating CIP in wastewater effluents for the benefit of humankind. Tsai *et al.* successfully designed a bifunctional Cu_xO/MOF in the presence of urea for the photocatalytic degradation of CIP under visible light in an aqueous medium.[43] This could serve as a potential and reliable candidate for establishing a new pathway for the advancement of visible-light-responsive photocatalysts to eliminate antibiotics and other emerging contaminants.

Again, *in situ* impregnation of $AgFeO_2$ into graphene and $Cu_2(BTC)_3$ MOF to synthesize tertiary heterojunction catalysts with efficiently engineered bandgap energies was demonstrated by El-Fawal and his team for utilization in the photocatalytic elimination of drug contaminants under irradiation of direct sunlight.[44] It was observed that the degradation efficiency of diclofenac was much greater than that of amoxicillin. The $AgFeO_2$/G@$Cu_2(BTC)_3$ heterojunction was investigated for the reclamation of real pharmaceutical wastewater effluent under direct sunlight to explore its practical applicability, achieving an excellent performance of 91%.

6. Mechanistic pathway

On exposure to light, the electrons present in the VB are excited to the CB, leaving behind the holes in the VB. These electrons and holes are responsible for the reduction and oxidation reactions in the photodegradation mechanism. Studies have demonstrated that the type-II band alignment in TiO_2@HKUST-1, as shown in Fig. 3(a) and (b), significantly speeds up the migration and separation of photo-generated charge carriers. To ensure complete contact of the pollutant molecule with TiO_2, the HKUST-1 shell adsorbs the molecule to the TiO_2@HKUST-1 cage.[24,26] This transfer of charges efficiently increases photocatalytic performance by successfully limiting the rate of recombination of the charge carriers.

The electron on the CB of HKUST-1 cannot interact with O_2 to produce $^{\bullet}O_2^-$ because the E_{CB}, which is 0.15 eV, is more active than the typical redox potential for $O_2/^{\bullet}O_2^-$, which is −0.33 eV *vs.* NHE. Additionally, the E_{VB} of HKUST-1 is observed to be 2.77 eV, which is more active than the standard redox potential of $^{\bullet}OH/OH^-$ (+1.99 eV *vs.* NHE). This suggests that the photogenerated h^+ in the VB can interact with H_2O/OH^- to produce $^{\bullet}OH$ radicals responsible for the degradation of the TC molecule. Moreover, the E_{VB} of TiO_2 is calculated to be 2.71 eV, which is much lower than the MOF. Hence, h^+ in the VB of the MOF migrates to the VB of TiO_2, subsequently reacting with H_2O/OH^- to create $^{\bullet}OH$ radicals for the decomposition mechanism. The following reactions demonstrate the degradation mechanism:

$$\text{HKUST-1} + h\nu \rightarrow \text{HKUST-1}\ (e^-) + \text{HKUST-1}\ (h^+) \quad (1)$$

$$\text{HKUST-1}\ (h^+) + H_2O \rightarrow {}^{\bullet}OH + H^+ + \text{HKUST-1} \quad (2)$$

$$^{\bullet}OH + \text{TC} \rightarrow \text{oxidization product} \quad (3)$$

$$TiO_2\ (h^+) + H_2O \rightarrow {}^{\bullet}OH + H^+ + TiO_2 \quad (4)$$

$$h^+ + \text{TC} \rightarrow \text{oxidization product} \quad (5)$$

An identical electron transfer pathway is displayed by the truncated octahedral Cu_2O@HKUST-1.[25] However, both the VB and CB of the octahedral Cu_2O are sandwiched inside the band gap of HKUST-1, leading to the recombination of

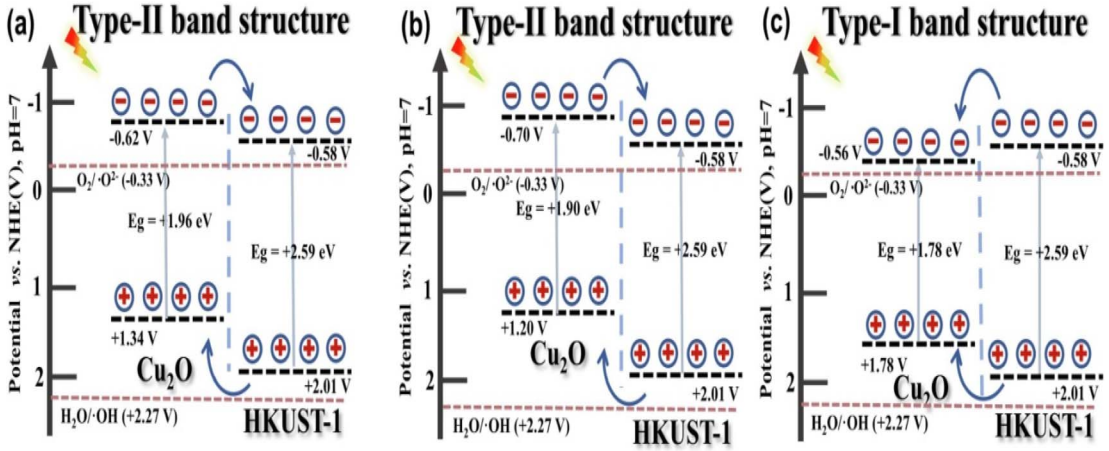

Fig. 3 The energy level illustration of (a) cubic, (b) truncated octahedral and (c) octahedral Cu_2O@HKUST-1. Reproduced from ref. 25.

photogenerated e^-–h^+ pairs (Fig. 3(c)). SnO_2/MOF-199, however, is observed to encourage the Z-scheme mechanism for the degradation of MZ molecules.[27,28] Here, the accumulation of the photogenerated e^-–h^+ is found to occur in the CB of the MOF and the VB of SnO_2. The accumulated e^- ions present in the CB of the MOF are more potent reducing agents than those present in the CB of SnO_2. In contrast, the h^+ ions collected in the VB of SnO_2 are better oxidizing agents than those present in the VB of MOF. These h^+ ions can efficiently oxidize the target pollutant molecules by generating $^{\bullet}OH$ radicals that are efficient ROS for photocatalytic degradation.[42] Small amounts of $^{\bullet}O_2^-$ radicals can also be generated in these systems by the accumulated e^- in the MOF-CB. However, $^{\bullet}O_2^-$ radicals and photogenerated electrons play a minor part in the breakdown of MZ molecules. The literature reports show that the photodegradation of MZ *via* the oxidation process is preferred over the reduction mechanism.

7. Influence of various parameters affecting overall degradation efficiency

The efficiency of a photocatalytic reaction is affected by various operational parameters besides the type of catalyst employed. Considering this, the effects of some of the essential factors are discussed below.

7.1. Photocatalyst loading

Owing to the increased formation of reactive radicals, the rate of photocatalytic degradation gradually increases as the amount of photocatalyst increases. However, the screening effect and light scattering cause a decrease in the rate of degradation in highly concentrated solutions. It can be observed in Fig. 4(a) that the degradation performance of TC-HCl is enhanced from 86.9% to 95.34% with an increase in the catalyst dosage from 0.05 to 0.10 g L^{-1}. However, when the catalyst loading of cubic Cu_2O@HKUST-1 was set to 0.40 g L^{-1}, the degradation efficiency decreased to 78.75%.[25,26] Similar results were obtained by Sheikhsamany *et al.*, and it was concluded that the degradation of MZ improved as the catalyst dosage increased, achieving an optimum loading of 2 g L^{-1}.[27] The observed results suggest that a higher dosage of the catalyst yields more reactive species during the photocatalytic reaction owing to the interaction of incident photons with the photocatalyst. However, the accumulation of excess catalysts increases the turbidity and opacity of the solution, thus minimizing light penetration and causing a substantial decrease in the degradation performance. Additionally, a major portion of the catalyst becomes inaccessible to molecules of the contaminants and incident radiation owing to the aggregation of the particles of the catalyst, which decreases the surface area at superior catalyst dosages.[28,45] Therefore, to improve photocatalytic degradation efficiency, determining ideal catalyst loading is a crucial factor.

7.2. Initial concentrations of pollutants

The efficiency of the photodegradation reaction decreases as the initial concentration of the contaminant increases, which may be caused by a reduction in the photonic efficiency and saturation of the active sites of the photocatalyst by the adsorbed molecules. Additionally, an increase in the initial concentration of the pollutant increases the concentration of the intermediate species, thereby saturating the active sites of the catalyst. Fig. 4(b) demonstrates that the degradation rate of TC-HCl was 92.81%, at an initial concentration of 20 mg L^{-1}, while the efficiency decreases with any further increase in the concentration of the pollutant. This can be attributed to the higher competition between pollutant molecules and intermediates for the active sites of the catalyst.[25,26] Moreover, high concentrations may impair photo-permeability and reduce the entry of surface photons. With a gradual increase in the concentration of MZ, more contaminant molecules are diffused to the surface of the photocatalyst, increasing the effectiveness of the interactions between the adsorbed molecules and $^{\bullet}OH$ radicals. Owing to their short lifetime, $^{\bullet}OH$ radicals had a lower possibility of interacting with the MZ molecules because the adsorbed molecules were insufficient at low concentrations. Consequently, they either rebonded or participated in secondary reactions.[46] The maximum collision probability was

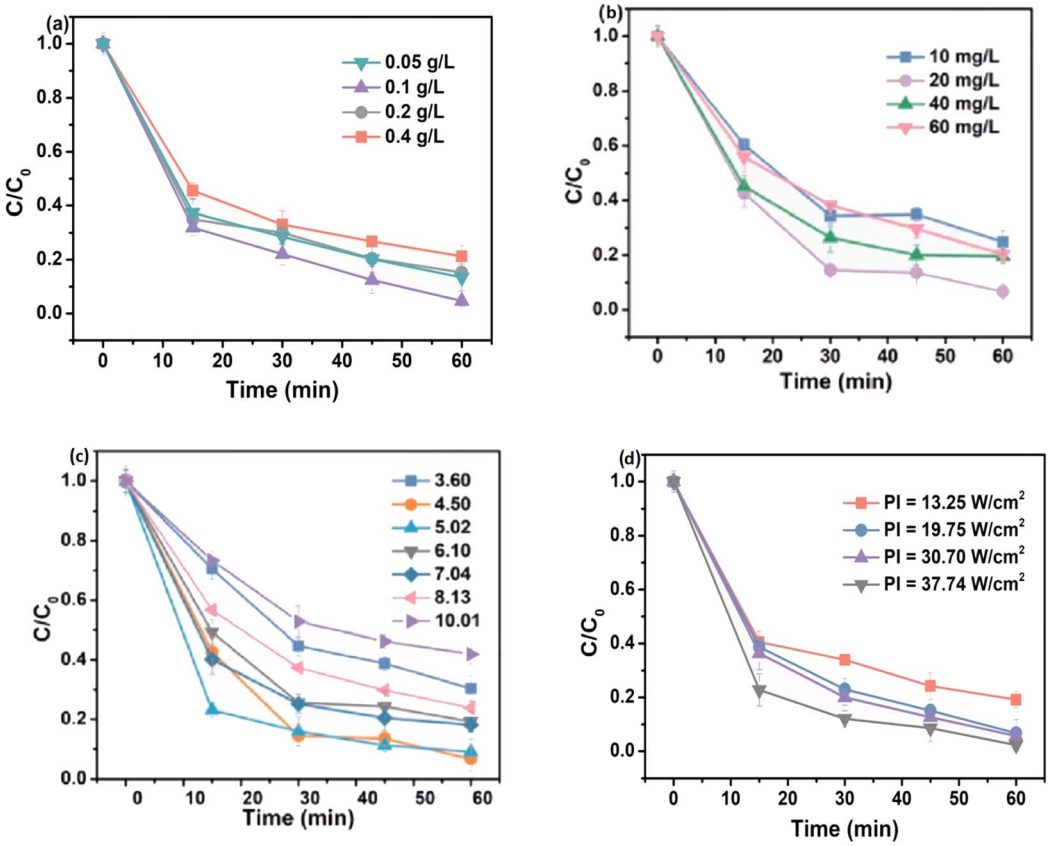

Fig. 4 Effect of different influencing factors on photocatalytic efficiency: (a) amount of catalyst; (b) initial pollutant concentration; (c) effect of pH; and (d) light intensity.

attained at the ideal concentration, which led to the highest photodegradation activity. Beyond this ideal concentration, contaminant molecules absorb a major part of the incident photons, thereby diminishing degradation performance.[27,28]

7.3. Influence of pH

pH is an important and determining factor that controls photocatalytic reactions. Modifying the charge of the photocatalyst surface and influencing particle aggregations can significantly affect the efficiency of degradation. Moreover, the acidity of the solution affects the electrostatic interactions between the surface of the photocatalyst, substrate and solvent molecules and charged reactive species. The point of zero charge (pH_{PZC}) of the catalyst is influenced by pH. The interactions between the surface of the photocatalyst and the substrate molecules are minimal at pH close to the pH_{PZC} value owing to the absence of electrostatic forces. However, at pH below pH_{PZC}, the positively charged surface of the photocatalyst electrostatically interacts with the negatively charged molecules, improving the degradation efficiency. The surface of the photocatalyst tends to be negatively charged at pH values higher than the pH_{PZC}, which repels and fends off the anionic molecules from the MOF surface.[27,28] To explore the effect of pH on the degradation of TC-HCl by cubic Cu_2O@HKUST-1, Wu *et al.* conducted experiments over a wide pH range between 3 and 10.[25,26] At pH values in the range of 3–10, the surface charge of the catalyst is found to be negative. As shown in Fig. 4(c), the electrostatic attraction between the positively charged TC-HCl molecules and the negatively charged surface of the nanocomposite favors an increase in degradation efficiency. However, an increase in the number of adsorbed pollutant molecules inhibits light radiation from reaching the catalyst surface, thereby reducing the light intensity at the surface and obstructing the photoexcitation process.

7.4. Wavelength and intensity of light

The intensity of light is one of the most crucial parameters affecting the photocatalytic process. A photocatalytic reaction requires a suitable reaction rate and electron–hole production, which is influenced by irradiation intensity. The wavelength and energy of irradiation influence the electronic and optical characteristics of the catalyst. The wavelength of light may generally be divided into three categories: UV, visible and solar. Considering this, the fabrication of semiconductors with lower band gaps that can be activated by light of higher wavelengths or lower energy, such as solar or visible light, has become an indispensable necessity. MOFs with narrower band gaps (E_g) can be activated by visible light. ZnO is activated by the irradiation of wavelengths shorter than 387 nm possessing E_g of 3.37 eV. To examine the intensity of light, four different light

Table 1 Different photocatalysts utilized for the photodegradation of pharmaceutical drugs from wastewater

Photocatalyst	Pharmaceutical	Conc. of pollutant (ppm)	Irradiation time (min)	Efficiency (%)	Ref.
ZnS-NiS/NC	MZ	4	150	69	47
ZnS-SnS_2/NC	MZ	2	250	84	48
N-doped TiO_2	TC-HCl	10	120	56.7	49
SnO_2-ZnO/NC	MZ	2	250	91	50
$MnFe_2O_4$/bio-char	TC-HCl	40	120	93	51
NiS-SnS_2/NC	MZ	3	270	90	52
NiO-ZnO/clionptilolite	MZ	1	150	88.5	53
CQDs/Bi_2WO_6/Cu_2O	TC-HCl	20	90	80	54
MoS_2@Fe_3O_4@Cu_2O	TC-HCl	20	90	70	55
Ag/AgCl@MIL-88(Fe)	Ibuprofen	10	210	93	56
g-C_3N_4/MIL-68(In)-NH_2	Ibuprofen	20	120	68	57
MIL-125ML/gCN	Cefixime	20	120	74	58
MIL-100(Fe)@Fe_3O_4/CA	TC-HCl	10	180	85	59
TiO_2@HKUST-1	TC-HCl	20	60	92.4	24
Cu_2O@HKUST-1	TC-HCl	20	60	94	26
SnO_2/MOF-199	MZ	40	240	80	27
$BaTi_{0.85}Zr_{0.15}O_3$/HKUST-1	TC-HCl	30	180	81.19	28

intensities ranging from 13.25 to 37.74 W cm^{-2} were used.[25] The rate of TC-HCl elimination improved from 80.84% to 97.80% with a gradual increase in the intensity of light, which can be attributed to the generation of a greater number of electron–hole pairs (Fig. 4(d)).

7.5. Dissolved O_2

By stabilizing intermediate radicals and preventing charge recombination effects, dissolved O_2 can directly influence the generation of intermediate species during photocatalytic mechanisms. Additionally, these dissolved molecules can directly contribute to the production of ROS, which are responsible for pollutant decomposition.

8. Comparison of Cu-MOFs with other photocatalysts

An evaluation of previously reported literature on the photocatalytic degradation of pharmaceuticals reveals that the efficiency of the Cu–BTC MOF is comparable to that reported in the literature, as presented in Table 1. As observed from table, HKUST-1 composites presented enhanced efficiency towards the degradation of high concentration (~40 ppm) pharmaceutical pollutants compared to other traditional photocatalysts, such as ZnO, TiO_2, ZnS, and MoS_2. The highest degradation efficiency was presented by HKUST-1 composites, such as Cu_2O@HKUST-1 and TiO_2@HKUST-1, which exhibited an interesting efficiency of 94% and 92.4% in just 60 min of 20 ppm solution of TC-HCl, respectively. This can be specifically attributed to the rapid recombination of photogenerated electron–hole pairs, low efficiency of solar energy utilization and limited surface-active sites of conventional semiconductors that hinder their photocatalytic efficiency. The Cu-MOF supports display exceptional properties of remarkable thermal stability, large surface area, and substantial pore volume. Notably, the presence of redox active Cu^{2+} ions enhances its effectiveness in photocatalysis by participating in both oxidation and reduction reactions. It also exhibits impressive structural integrity during the adsorption–desorption of water. Moreover, the easy synthesis procedure of Cu-BTC MOFs, such as SnO_2-MOF composite, makes it a promising candidate for photocatalytic applications.

9. Conclusion and future outlook

The tunable porosity and excellent specific surface area of MOFs make them broadly integrated with other hybrid materials for designing more effective and promising composite photocatalysts. It compensates for limitations, such as poor response to visible light and a higher recombination rate of photogenerated electrons and holes. These characteristics make them superior to other materials and a current attractive topic of study among researchers working in the field of photocatalysis to eliminate contaminants from the aqueous phase. To address the needs of photocatalytic activity, designing novel MOF composites by tailoring organic ligands has become key to research. This study summarizes the most recent advancements in the utilization of MOF-199 in the remediation of wastewater effluents contaminated with pharmaceutical pollutants. However, in-depth research is essential to evaluate the applicability of the photocatalytic performance of the MOF composite in real-time practical wastewater compared to that in laboratory environment simulation. The majority of reported studies have focused on the laboratory application of MOFs for the photocatalytic degradation of water pollutants. However, it is essential to scale up for practical industrial water treatment applications, which call for more simple, reliable and cost-effective material synthesis techniques. Moreover, stability and recyclability are other crucial aspects to consider for a sustainable large-scale utility. Therefore, the fabrication of high-performance photocatalysts to be employed under

aqueous and acidic conditions is still a key component in achieving the advancement of MOF-based photocatalysts. Simultaneously, integrating MOFs with non-metals, nanomaterials and carbon-based materials as an alternative to precious metals might be a viable choice in the future for further enhancing their photocatalytic performance.

However, despite such drawbacks, research on MOF-based materials is currently exploding across many disciplines, particularly in photocatalytic engineering, highlighting the potential and room for developing MOF-based photocatalysts. It is anticipated that with continued research and exploration, MOF-based photocatalysts offer innovative approaches and strategies for the degradation of water-phase organic pollutants for the achievement of sustainable development.

Conflicts of interest

There are no conflicts to declare.

References

1 K. P. Gopinath, N. V. Madhav, A. Krishnan, R. Malolan and G. Rangarajan, *J. Environ. Manage.*, 2020, **270**, 110906.
2 N. A. Nordin, M. A. Mohamed, M. N. I. Salehmin and S. F. M. Yusoff, *Coord. Chem. Rev.*, 2022, **468**, 214639.
3 S. R. Mishra, V. Gadore and M. Ahmaruzzaman, *Environ. Nanotechnol., Monit. Manage.*, 2023, **20**, 100807.
4 S. Roy and M. Ahmaruzzaman, *J. Environ. Manage.*, 2022, **315**, 115089.
5 G. K. Yadav and M. Ahmaruzzaman, *J. Nanopart. Res.*, 2021, **23**, 213.
6 J. E. Cun, X. Fan, Q. Pan, W. Gao, K. Luo, B. He and Y. Pu, *Adv. Colloid Interface Sci.*, 2022, **305**, 102686.
7 M. Mon, R. Bruno, J. Ferrando-Soria, D. Armentano and E. Pardo, *J. Mater. Chem. A*, 2018, **6**, 4912–4947.
8 S. Roy, J. Darabdhara and M. Ahmaruzzaman, *Environ. Sci. Pollut. Res.*, 2023, 1–19.
9 Z. U. Zango, K. Jumbri, N. S. Sambudi, A. Ramli, N. H. H. Abu Bakar, B. Saad, M. N. H. Rozaini, H. A. Isiyaka, A. H. Jagaba, O. Aldaghri and A. Sulieman, *Polymers*, 2020, **12**, 2648.
10 T. Xia, Y. Lin, W. Li and M. Ju, *Chin. Chem. Lett.*, 2021, **32**, 2975–2984.
11 S. Gautam, H. Agrawal, M. Thakur, A. Akbari, H. Sharda, R. Kaur and M. Amini, *J. Environ. Chem. Eng.*, 2020, **8**, 103726.
12 D. Mukherjee, B. Van der Bruggen and B. Mandal, *Chemosphere*, 2022, **295**, 133835.
13 Y. C. Lopez, H. Viltres, N. K. Gupta, P. Acevedo-Pena, C. Leyva, Y. Ghaffari, A. Gupta, S. Kim, J. Bae and K. S. Kim, *Environ. Chem. Lett.*, 2021, **19**, 1295–1334.
14 Z. Zhang, L. Bian, H. Tian, Y. Liu, Y. Bando, Y. Yamauchi and Z. L. Wang, *Small*, 2022, **18**, 2107450.
15 A. Domán, S. Klébert, J. Madarász, G. Sáfrán, Y. Wang and K. László, *Nanomater*, 2020, **10**, 1182.
16 M. Luo, J. Yang, X. Li, M. Eguchi, Y. Yamauchi and Z. L. Wang, *Chem. Sci.*, 2023, **14**, 3400–3414.
17 Z. Y. Zhang, H. Tian, L. Bian, S. Z. Liu, Y. Liu and Z. L. Wang, *J. Energy Chem.*, 2023, **83**, 90–97.
18 R. Singh, G. Singh, N. George, G. Singh, S. Gupta, H. Singh, G. Kaur and J. Singh, *Catalysts*, 2023, **13**, 130.
19 D. Yang, Y. Chen, Z. Su, X. Zhang, W. Zhang and K. Srinivas, *Coord. Chem. Rev.*, 2021, **428**, 213619.
20 M. Bagheri, A. Melillo, B. Ferrer, M. Y. Masoomi and H. Garcia, *ACS Appl. Mater. Interfaces*, 2021, **14**, 978–989.
21 C. Yue, L. Chen, H. Zhang, J. Huang, H. Jiang, H. Li and S. Yang, *Environ. Sci. Water Res. Technol.*, 2023, **9**, 669–695.
22 A. Domán, J. Madarász, G. Sáfrán, Y. Wang and K. László, *Microporous Mesoporous Mater.*, 2021, **316**, 110948.
23 Y. Liu, P. Ghimire and M. Jaroniec, *J. Colloid Interface Sci.*, 2019, **535**, 122–132.
24 Y. Qiao, C. Sun, J. Jian, T. Zhou, X. Xue, J. Shi, G. Che and G. Liao, *J. Mol. Liq.*, 2023, 122383.
25 Y. Wu, Y. Li, H. Li, H. Guo, Q. Yang and X. Li, *Sep. Purif. Technol.*, 2022, **303**, 122106.
26 Y. Wu, X. Li, H. Zhao, F. Yao, J. Cao, Z. Chen, D. Wang and Q. Yang, *Chem. Eng. J.*, 2021, **426**, 131255.
27 R. Sheikhsamany, H. Faghihian and R. Fazaeli, *Mater. Sci. Semicond.*, 2022, **138**, 106310.
28 R. Sheikhsamany, H. Faghihian and R. Fazaeli, *Inorg. Chem. Commun.*, 2021, **134**, 109048.
29 Y. Xiong, F. Ye, C. Zhang, S. Shen, L. Su and S. Zhao, *RSC Adv.*, 2015, **5**, 5164–5172.
30 E. M. C. Morales, M. A. Méndez-Rojas, L. M. Torres-Martínez, L. F. Garay-Rodríguez, I. López, I. E. Uflyand and B. I. Kharisov, *Polyhedron*, 2021, **210**, 115517.
31 F. A. Sofi, K. Majid and O. Mehraj, *J. Alloys .Compd*, 2018, **737**, 798–808; F. Zou, R. Yu, R. Li and W. Li, *ChemPhysChem.*, 2013, **14**, 2825–2832.
32 C. McKinstry, E. J. Cussen, A. J. Fletcher, S. V. Patwardhan and J. Sefcik, *Chem. Eng. J.*, 2017, **326**, 570–577.
33 G. Blanita, G. Borodi, M. D. Lazar, A. R. Biris, L. Barbu-Tudoran, I. Coldea and D. Lupu, *RSC Adv.*, 2016, **6**, 25967–25974.
34 M. R. Armstrong, S. Senthilnathan, C. J. Balzer, B. Shan, L. Chen and B. Mu, *Ultrason. Sonochem.*, 2017, **34**, 365–370.
35 J. Vehrenberg, M. Vepsäläinen, D. S. Macedo, M. Rubio-Martinez, N. A. Webster and M. Wessling, *Microporous Mesoporous Mater.*, 2020, **303**, 110218.
36 H. Ren and T. Wei, *ChemElectroChem*, 2022, **9**, e202200196.
37 M. Bellusci, A. Masi, M. Albino, D. Peddis, M. Petrecca, C. Sangregorio, A. La Barbera and F. Varsano, *Microporous Mesoporous Mater.*, 2021, **328**, 111458.
38 Y. Li, J. Miao, X. Sun, J. Xiao, Y. Li, H. Wang, Q. Xia and Z. Li, *Chem. Eng. J.*, 2016, **298**, 191–197.
39 N. Faaizatunnisa, R. Ediati, H. Fansuri, H. Juwono, S. Suprapto, A. R. P. Hidayat and L. L. Zulfa, *Nano-Struct. Nano-Objects*, 2023, **34**, 100968.
40 Y. Luo, G. Huang, Y. Li, Y. Yao, J. Huang, P. Zhang, S. Ren, J. Shen and Z. Zhang, *Sci. Total Environ.*, 2023, **857**, 159279.
41 P. H. Andrade, A. L. Gomes, H. G. Palhares, C. Volkringer, A. Moissette, H. F. Victória, N. M. Hatem, K. Krambrock, M. Houmard and E. H. Nunes, *J. Mater. Sci.*, 2022, **57**, 4481–4503.

42 L. Yuan, Z. Wang and F. Gu, *J. Environ. Chem. Eng.*, 2022, **10**, 107964.
43 C. K. Tsai, C. H. Huang, J. J. Horng, H. L. Ong and R. A. Doong, *Nanomater*, 2023, **13**, 282.
44 E. M. El-Fawal, S. A. Younis and T. Zaki, *J. Photochem. Photobiol., A*, 2020, **401**, 112746.
45 A. Nezamzadeh-Ejhieh and H. Zabihi-Mobarakeh, *J. Ind. Eng. Chem.*, 2014, **20**, 1421–1431.
46 F. Zahedi, M. Behpour, S. M. Ghoreishi and H. Khalilian, *Sol. Energy*, 2015, **120**, 287–295.
47 H. Derikvandi and A. Nezamzadeh-Ejhieh, *J. Colloid Interface Sci.*, 2017, **490**, 652–664.
48 H. Derikvandi and A. Nezamzadeh-Ejhieh, *J. Photochem. Photobiol., A*, 2017, **348**, 68–78.
49 S. Wu, H. Hu, Y. Lin, J. Zhang and Y. H. Hu, *Chem. Eng. J.*, 2020, **382**, 122842.
50 H. Derikvandi and A. Nezamzadeh-Ejhieh, *J. Mol. Catal. A: Chem.*, 2017, **426**, 158–169.
51 C. Lai, F. Huang, G. Zeng, D. Huang, L. Qin, M. Cheng, C. Zhang, B. Li, H. Yi, S. Liu and L. Li, *Chemosphere*, 2019, **224**, 910–921.
52 H. Derikvandi and A. Nezamzadeh-Ejhieh, *J. Colloid Interface Sci.*, 2017, **490**, 628–641.
53 H. Derikvandi and A. Nezamzadeh-Ejhieh, *J. Hazard. Mater.*, 2017, **321**, 629–638.
54 Y. Yang, Z. Zhu, Z. Liu, H. J. Dong, Y. Liu, M. B. Wei, P. W. Huo, C. X. Li and Y. S. Yan, *J. Taiwan Inst. Chem. Eng.*, 2019, **102**, 197–201.
55 W. J. Li, G. S. Zhou, X. D. Zhu, M. S. Song, P. P. Wang, C. C. Ma, X. L. Liu, S. Han, Y. Q. Huang and Z. Y. Lu, *Appl. Surf. Sci.*, 2021, **555**, 149730.
56 W. Huang, C. Jing, X. Zhang, M. Tang, L. Tang, M. Wu and N. Liu, *Chem. Eng. J.*, 2018, **349**, 603–612.
57 L. L. Yu, W. Cao, S. C. Wu, C. Yang and J. H. Cheng, *Ecotoxicol. Environ. Saf.*, 2018, **164**, 289–296.
58 M. Salimi, A. Esrafili, A. J. Jafari, M. Gholami, H. R. Sobhi, M. Nourbakhsh and B. Akbari-Adergani, *Colloids Surf., A*, 2019, **582**, 123874.
59 H. U. Rasheed, X. Lv, S. Zhang, W. Wei and J. Xie, *Adv. Powder Technol.*, 2018, **29**, 3305–3314.